

Abstract

The global extent of agriculture demands a thorough understanding of the ways it impacts the Earth system through both the modification of the physical and biological characteristics of the landscape as well as through emissions of greenhouse gases and aerosols. People use fire to manage cropland and pasture in many parts of the world, impacting both the timing and amount of fire. So far, much previous research into how these land uses affect fire regimes has either focused on individual small regions or global patterns at annual or decadal scales. Moreover, because pasture is not mapped globally at high resolution, the amount of fire associated with pasture has never been quantified as it has for cropland. The work presented here resolves the effects of agriculture – including pasture – on fire on a monthly basis for regions across the world, using globally gridded data on fire activity and land use at 0.25° resolution. The first global estimate of pasture-associated fire reveals that it accounts for over 40 % of annual burned area. Cropland, generally assumed to reduce fire occurrence, is shown to enhance or suppress fire at different times of year within individual regions. These results bridge important gaps in the understanding of how agriculture and associated management practices influence vegetation fire, enabling the next generation of vegetation and Earth system models more realistically incorporate these anthropogenic effects.

1 Introduction

Vegetation fire is a worldwide phenomenon with consequences for the biosphere, atmosphere, climate, and human health. Annual emissions of carbon (in various chemical forms) from fire have been estimated at 2.5 Pg yr^{-1} (2001–2009; Randerson et al., 2012). The radiative forcing from the black carbon emitted from fires since 1750 has been estimated to be 0.2 W m^{-2} , which is about equivalent to 12 % of radiative forcing due to the accumulated anthropogenic CO_2 over the same time period (Bond et al.,

BGD

12, 10817–10855, 2015

Quantifying regional, time-varying effects of cropland

S. S. Rabin et al.

Title Page

Abstract

Introduction

Conclusions

References

Tables

Figures



Back

Close

Full Screen / Esc

Printer-friendly Version

Interactive Discussion



mapped by satellite as cropland has, no global estimates of pasture burning have ever been produced. This means that estimates of pasture and non-agricultural fire are entangled in global datasets, and thus observations have not distinguished what may be important differences in fire regime. To understand the total effect of agricultural management on fire occurrence, then, the scientific community must go beyond estimates of cropland burned area and associated emissions.

The work presented here is an effort to bridge these gaps in our knowledge. We present a method that uses fire observations in conjunction with estimates of land-use distribution to statistically estimate the amount of fire associated with cropland, pasture, and other lands at global and regional scales. In addition to examining the total area of such burning, the same method is used to investigate patterns of associated carbon emissions.

2 Methods

2.1 Analytical technique

Magi et al. (2012) analyzed seasonal patterns of agricultural burning (i.e., combined cropland and pasture) from non-agricultural burning using estimates of land-use distributions and satellite-derived fire data. This study builds upon the methods presented by Magi et al. (2012), differentiating among cropland, pasture, and other burning and generating estimates of the amount of each type of fire in terms of both burned area and carbon emissions.

The total amount of burned area in some grid cell i (B_i) can be represented as the sum of the burned area on each land-use type k . This can in turn be represented as the product of the area of that land cover type in the grid cell ($A_{k,i}$) and the fraction of that land-use type that burned in that grid cell ($F_{k,i}$):

$$B_i = F_{c,i}A_{c,i} + F_{p,i}A_{p,i} + F_{o,i}A_{o,i}$$

Quantifying regional, time-varying effects of cropland

S. S. Rabin et al.

Title Page

Abstract

Introduction

Conclusions

References

Tables

Figures



Back

Close

Full Screen / Esc

Printer-friendly Version

Interactive Discussion



where the subscripts c, p, and o refer to cropland, pasture, and other land, respectively. The values of each $F_{k,i}$ are unknown, but a best-guess \widehat{F}_k can be estimated across a group of N grid cells:

$$\begin{bmatrix} B_1 \\ B_2 \\ \vdots \\ B_i \\ \vdots \\ B_N \end{bmatrix} = \begin{bmatrix} A_{c1} & A_{p1} & A_{o1} \\ A_{c2} & A_{p2} & A_{o2} \\ \vdots & \vdots & \vdots \\ A_{ci} & A_{pi} & A_{oi} \\ \vdots & \vdots & \vdots \\ A_{cN} & A_{pN} & A_{oN} \end{bmatrix} \times \begin{bmatrix} \widehat{F}_{c,i} \\ \widehat{F}_{p,i} \\ \widehat{F}_{o,i} \end{bmatrix} + \begin{bmatrix} \epsilon_1 \\ \epsilon_2 \\ \vdots \\ \epsilon_i \\ \vdots \\ \epsilon_N \end{bmatrix}$$

$$5 \quad \mathbf{B} = \mathbf{A}\widehat{\mathbf{F}} + \boldsymbol{\epsilon}$$

where ϵ_i is the residual for grid cell i . The set of \widehat{F}_k values that minimize the sum of squared errors across a large number of grid cells can be calculated using

$$\widehat{\mathbf{F}} = (\mathbf{A}^T\mathbf{A})^{-1}\mathbf{A}^T\mathbf{B}$$

10 where \mathbf{A} and \mathbf{B} are observations of land-use distributions and burned area, respectively. We have observed that a number of \widehat{F}_k values are found to be negative. This has two possible interpretations. One is that negative \widehat{F}_k values are simply a statistical artifact of the analysis without physical meaning, and that such lands either burn very little or not at all. The other possibility is that negative \widehat{F}_k values represent a real aspect of fire occurrence: namely, that the negative influence of such land covers on other
 15 land covers outweighs any fire happening on the land cover itself. For the purposes of illustration, consider a hypothetical grid cell for which the analysis estimates 5 km² of burned area for cropland:

$$F_{c,i}A_{c,i} = 5$$

$$B_i = F_{c,i}A_{c,i} + F_{p,i}A_{p,i} + F_{o,i}A_{o,i}$$

Quantifying regional, time-varying effects of cropland

S. S. Rabin et al.

Title Page	
Abstract	Introduction
Conclusions	References
Tables	Figures
◀	▶
◀	▶
Back	Close
Full Screen / Esc	
Printer-friendly Version	
Interactive Discussion	



A different grid cell with equal \widehat{F}_k values and twice the area of cropland but the same amounts of pasture and other land would have 5 km² more burning estimated:

$$F_{c,i}(2A_{c,i}) + F_{p,i}A_{p,i} + F_{o,i}A_{o,i} = B_i + F_{c,i}A_{c,i} = B_i + 5$$

The same logic shows that there would be less fire in the second grid cell if \widehat{F}_c were negative.

Conversely, \widehat{F}_k values could also incorporate positive effects of one land-use type on the others. For example, much of the fire observed in the frontier of the Amazon rainforest is associated with land management burning that escapes into surrounding forest (Uhl and Buschbacher, 1985; Cochrane and Schulze, 1998). The \widehat{F}_c and \widehat{F}_p values in that region could potentially account for this effect as well. In this conceptualization, then, \widehat{F}_k values should be interpreted not as “the fraction of land use k that burns across the region,” but rather as “the net effect of land use k on fire in the region, expressed as a fraction of the area of land use k in the region.”

The results presented in this study are explored in the main text with this latter interpretation of \widehat{F}_k values in mind. Appendix A shows results with \widehat{F}_k restricted to positive values, essentially interpreting \widehat{F}_k values as “the fraction of land use k that burns across the region.”

To account for temporal variability in the total amount of fire and its distribution among different land-use types, the analysis is performed separately for each month and year. Fire patterns and practices also vary across space, so each of 132 regions is analyzed separately. This set of regions (Fig. 1) was created with the goal of minimizing within-region heterogeneity in terms of climate, biome, and fire extent and timing, while still including enough grid cells to ensure an adequate sample size for estimation. The final region set resulted from an iterative process whereby we performed the analysis for a candidate region set, noted areas of severe under- or over-estimation, drew new region boundaries, and re-ran the analysis. The Terrestrial Ecosystems of the World map (Olson et al., 2001), agricultural distribution maps (Klein Goldewijk et al., 2010), and observations of fire extent and timing (Randerson et al., 2012) guided development

Quantifying regional, time-varying effects of cropland

S. S. Rabin et al.

Title Page

Abstract

Introduction

Conclusions

References

Tables

Figures



Back

Close

Full Screen / Esc

Printer-friendly Version

Interactive Discussion



as pasture (Randerson et al., 2012). Results for cropland influence on burned area from this analysis are compared to GFED3s estimates of burned area on cropland as well as “cropland-natural mosaic,” which is defined as land with “a mosaic of croplands, forests, shrubland, and grasslands in which no one component comprises more than 60 % of the landscape” (Friedl et al., 2002).

GFED3s estimates of fire-related emissions were generated by coupling the burned area observations for each land-use type with a climate-driven vegetation model (Randerson et al., 2012). Biome-specific emissions factors combined with biomass estimates from the vegetation model then produced the amount of emissions per area burned. The analytical technique described in Sect. 2.1 can be as easily applied to emissions as it can to burned area, in which case the \widehat{F}_k values represent the net effect per square kilometer of each land-use type on fire emissions. Here, an analysis of emissions of carbon-containing compounds was conducted in parallel with the analysis of burned area. A breakdown of GFED3s carbon emissions by land cover type, such as was provided for burned area, was not available.

2.2.2 Land use

Data on area of cropland and pasture were taken from an annualized version of the History Database of the Global Environment version 3.1 (HYDEV3.1), described by Klein Goldewijk et al. (2010). This public dataset, available at 5 min spatial resolution, is the basis for the historical part of the standardized gridded land-use transitions reconstructions (Hurtt et al., 2011) used in the Coupled Model Intercomparison Project, phase 5 (Taylor et al., 2012). The publicly available data are only produced for every five years during the recent past, but K. Klein Goldewijk provided annual estimates for the period 2000–2009 (personal communication, 2012). Distributions are assumed to not change within years. The amount of “other” (“non-agricultural”) land is calculated as the fraction of land not classified as cropland or pasture.

Grazing land can take many different forms, including both planted forage species and naturally occurring species (often referred to as rangeland). Data from the Food

BGD

12, 10817–10855, 2015

Quantifying regional, time-varying effects of cropland

S. S. Rabin et al.

Title Page

Abstract

Introduction

Conclusions

References

Tables

Figures



Back

Close

Full Screen / Esc

Printer-friendly Version

Interactive Discussion



fraction combusted (Seiler and Crutzen, 1980). Fuel load should be higher on average for non-agricultural lands than for pasture because pastures do not have trees in densities comparable to more carbon-rich forest ecosystems. Moreover, although croplands had a net positive contribution to global burned area, they had a net negative effect on fire emissions (Fig. 2). This suggests that, even though less area would have burned with less cropland, the burning would be happening in more carbon-dense ecosystems. As with burned area, total global fire emissions were very slightly overestimated (by less than 0.4 %; Fig. 2b).

Figure 3 shows time series plots as in Fig. 2, but broken down by GFED region. Pasture can be seen to account for a sizeable portion of burning in South America (NHSA and SHSA), Africa (NHAF and SHAF), Central Asia (CEAS), and Australia (AUST). Overall, the algorithm reproduces the amount and interannual variability of total fire well at these large regional scales. The most apparent discrepancies compared to GFED3s occur in Europe (EURO) and the Middle East (MIDE), whose mean annual burned area totals are underestimated by ~ 40 and ~ 30 %, respectively. With respective mean annual observed burned areas of $\sim 11\,200$ and $\sim 15\,800$ km² (0.2 and 0.3 % of global fire activity), however, these are the least-burned GFED regions.

The net mean annual burned area associated with croplands, pasture, and other land is illustrated in the maps in Fig. 4. Pasture accounts for a large amount of burned area in the savannas of NHAF and SHAF, with NHSA, SHSA, CEAS, and AUST being highlighted to a lesser degree. Eastern Europe, northern Australia, various parts of sub-Saharan Africa, and especially India's Punjab state emerge as spots where cropland has a strong positive effect on burned area (Fig. 4a). Cropland has a net negative effect on burned area in other places – most notably Cambodia and southern Vietnam, Ethiopia and South Sudan, India, eastern Argentina, and southeastern Australia. These are mostly biomes where vegetation tends to be quite fire-prone, and thus where strong active and/or passive suppression due to cropland might be expected. Interestingly, pasture and non-agricultural lands are also seen to sometimes have net suppressive effects (Fig. 8b and c). In the case of pasture, this could be due to a pas-

BGD

12, 10817–10855, 2015

Quantifying regional, time-varying effects of cropland

S. S. Rabin et al.

Title Page

Abstract

Introduction

Conclusions

References

Tables

Figures



Back

Close

Full Screen / Esc

Printer-friendly Version

Interactive Discussion



BGD

12, 10817–10855, 2015

**Quantifying regional,
time-varying effects
of cropland**

S. S. Rabin et al.

[Title Page](#)[Abstract](#)[Introduction](#)[Conclusions](#)[References](#)[Tables](#)[Figures](#)[Back](#)[Close](#)[Full Screen / Esc](#)[Printer-friendly Version](#)[Interactive Discussion](#)

South America (NHSA) and Equatorial Asia (EQAS) – cropland has an apparent negative influence on burned area for several months of the year. A comparison with observed cropland burning (of which there is little in such months) suggests that this is often a nearly pure signal of a suppressive effect. The effect appears especially strong in EQAS during September and October, although the large amount of cropland-natural mosaic burning complicates interpretation there. Pasture sometimes has a similar effect, although rarely; this is most apparent in TENA, EURO, MIDE, and SEAS. In EURO and CEAS, even other lands sometimes have a net negative estimated burned area. As discussed above, negative influence of pasture and non-agricultural lands could reflect active and/or suppressive effects associated with these land use/cover types.

The effect of different land uses on fire can be best explored and understood by examining patterns across a few regions. The savannas of western Africa have seen a good deal of remote sensing, anthropological, and ecological research regarding their fire regimes and thus provide a good example. The Sudanian savanna there experiences a distinct dry season from approximately October or November through April or May, during which it burns extensively (Laris, 2002; Kull and Laris, 2009). The fire regime is highly managed by people for agriculture and other purposes, with burning generally initiated early in the dry season and suppressed later. Early fires can have a number of benefits. For example, burning that occurs while the soil still has some residual moisture allows herbaceous regrowth, replenishing food availability for livestock ahead of the worst of the dry season (Mbow et al., 2000). Due to higher fuel moisture, these fires are also often easier to control than more intense burns under more flammable conditions later in the dry season. People often burn savanna early to fragment the burnable landscape, preventing late-season burns that can damage property and resources (Laris, 2002).

We isolated three regions (Fig. 7a) that mostly fall into the ecoregions “West Sudanian savanna” and “Guinean forest-savanna mosaic” according to Olson et al. (2001). Small amounts of other land cover types – including lowland and montane forests, flooded savanna, and Sahelian acacia savanna – are also included. On average, this

area sees a slight negative annual contribution of cropland to burned area; pasture contributes over a third of the observed annual burned area, with non-agricultural lands accounting for approximately twice that. Observed total burned area, which is matched almost perfectly by the estimate, peaks with pasture and non-agricultural burning in December (Fig. 7). As expected based on the literature on human fire management practices in this region (Mbow et al., 2000; Laris, 2002), most fire associated with pasture and non-agricultural land occurs in the early dry season – i.e., before January. Interestingly, though, the fire season for pasture seems to begin and end about a month earlier than that of non-agricultural land: from about October through January instead of November through February. Although early fire is often beneficial for all savanna in the region, the added impetus of burning early to create food for livestock appears to result in a distinct pattern. An overall net suppressive effect of cropland is also evident, with the strongest negative influence corresponding to the December peak of non-cropland fire. This emerges despite the fact that at least some cropland burning (including cropland-natural mosaic) was observed throughout the dry season (Fig. 7). Even though there is some observed fire associated with cropland, then, there would be much more if cropland were replaced with pasture or non-agricultural land. This interpretation has assumed that negative values are meaningful, but similar patterns emerge using constrained \widehat{F}_k values (Fig. A6).

4 Discussion

4.1 First estimates of pasture-associated fire

Pasture fire accounts for about 43 % of global annual burned area and about 22 % of global C emissions from fire. Pasture burning is especially important in CEAS, NHSA, NHAf, SHAF, and SHSA, in each of which it accounts for over 40 % of annual burned area. These regions together comprise 81 % of mean annual burning. As with the global numbers, the fraction of annual fire emissions from pasture burning there is disproportional.

BGD

12, 10817–10855, 2015

Quantifying regional, time-varying effects of cropland

S. S. Rabin et al.

Title Page

Abstract

Introduction

Conclusions

References

Tables

Figures



Back

Close

Full Screen / Esc

Printer-friendly Version

Interactive Discussion



5 icant advance over previous methods (Klein Goldewijk et al., 2007, 2010). However, the FAO numbers themselves may not be completely internally consistent, since they are compiled and reported by each country. A wide variety of ecosystem types and land-use patterns might all qualify as what the FAO terms “permanent pasture,” and countries’ standards of what to report likely differ (Klein Goldewijk et al., 2007). Differing methods of compilation introduce another source of uncertainty.

10 By incorporating active fire detections as an ancillary source of “burned area” information, the algorithm used in GFED3s was designed to avoid (as much as possible) the issue of fires much smaller than a single sensor pixel being excluded (Randerson et al., 2012). Even though GFED3s includes much more cropland fire than GFED3, it likely still misses much such burning. For example, McCarty et al. (2009) used field-work to inform a remote sensing estimate of cropland burning in the contiguous US and found that an average of more than 1.2 Mha yr^{-1} burned between 2003 and 2007; during the same period, GFED3s has only 0.67 Mha yr^{-1} (or 0.93 Mha yr^{-1} if also including cropland-natural mosaic). Moreo-
15 ver, the “small fires” improvement may not have improved the detection of burning underneath a relatively undamaged canopy, which poses a challenge even for active fire sensors and algorithms (Giglio, 2013). In regions of southern Africa with tree cover $\geq 21\%$, this was blamed for a 41% underestimate of burned area in an assessment of the algorithm underlying most of GFED3 (Giglio et al., 2009); a similar assessment has not been performed for GFED3s.
20

4.3 Impacts of regional analysis

25 The specific set of regions chosen for this analysis can be important for the quality of the results. One aspect to consider is that analysis regions that are too extensive may encompass too many different fire patterns for any one set of \widehat{F}_k values to describe well. This may have been the cause of the poor performance in EURO and MIDE with regard to total fire (Fig. 3): both include parts of one or more very large analysis regions (Fig. 1), which if broken down into more fine-grained regions would likely better account for heterogeneity in fire patterns and practices. Large analysis regions are

Quantifying regional, time-varying effects of cropland

S. S. Rabin et al.

Title Page

Abstract

Introduction

Conclusions

References

Tables

Figures



Back

Close

Full Screen / Esc

Printer-friendly Version

Interactive Discussion



not necessarily detrimental, however – Boreal Asia (BOAS) has several (Fig. 1) but is relatively well described (Fig. 3).

Another, more general consequence of the regional analysis is that spatial heterogeneity of burning within analysis regions is not well represented in the results. As expected based on the mathematics involved in the parameterization, the total estimated amount of fire at the regional level is usually quite accurate (Fig. 8a) – estimated total burned area was correct to within 5 in 86% of region-months with fire observed. However, there is a large amount of scatter when comparing observed vs. estimated burned area for individual grid cells (Fig. 8b). Especially noticeable is the large number of grid cells with zero (or very little) observed fire that are overestimated by the algorithm. The maps in Fig. 5 illustrate this problem in a more intuitive format. Although fire activity is usually well characterized at the level of the analysis region (as illustrated by Fig. 8a), Figure 5 shows that it does not fully incorporate the heterogeneity evident in the observations. Thus, interpretations of the maps in Fig. 4 should focus on general patterns without delving too deeply into gridcell-by-gridcell variation.

Finally, because the GFED region boundaries do not all correspond to those of the analysis regions, GFED regions without much fire are highly sensitive to inclusion of parts of analysis regions with too much or too little estimated fire. This also may have contributed to the poor performance in EURO and MIDE (Fig. 3). For example, Afghanistan (MIDE) is included in analysis region 26, “West-central Asian desert steppe” (AR26), which is not completely contained by MIDE. Afghanistan is an area of overestimate in AR26, and although it is balanced out by underestimates elsewhere in that region (especially along its northern boundary), MIDE only includes the overestimate. This effect, then, contributes to the net overestimate in MIDE.

5 Conclusions

The analysis presented here shows that agriculture does have far-reaching consequences on vegetation fire, often in ways not previously measured or considered at

BGD

12, 10817–10855, 2015

Quantifying regional, time-varying effects of cropland

S. S. Rabin et al.

Title Page

Abstract

Introduction

Conclusions

References

Tables

Figures



Back

Close

Full Screen / Esc

Printer-friendly Version

Interactive Discussion



Kees Klein Goldewijk for sharing annual HYDE data, and James Randerson for granting early access to the GFED3s dataset.

References

- Andela, N. and van der Werf, G. R.: Recent trends in African fires driven by cropland expansion and El Niño to La Niña transition, *Nature Climate Change*, 4, 791–795, 2014. 10819, 10834
- Archibald, S., Roy, D. P., van Wilgen, B. W., and Scholes, R.: What limits fire? An examination of drivers of burnt area in Southern Africa, *Glob. Change Biol.*, 15, 613–630, 2008. 10819, 10820, 10834
- Archibald, S., Staver, A. C., and Levin, S. A.: Evolution of human-driven fire regimes in Africa, *P. Natl. Acad. Sci. USA*, 109, 847–852, 2012. 10819
- Archibald, S., Lehmann, C. E. R., Gomez-Dans, J. L., and Bradstock, R. A.: Defining pyromes and global syndromes of fire regimes, *P. Natl. Acad. Sci. USA*, 110, 6442–6447, 2013. 10819
- Arora, V. K. and Boer, G.: Fire as an interactive component of dynamic vegetation models, *J. Geophys. Res.*, 110, 1–20, 2005. 10820
- Bistinas, I., Harrison, S. P., Prentice, I. C., and Pereira, J. M. C.: Causal relationships versus emergent patterns in the global controls of fire frequency, *Biogeosciences*, 11, 5087–5101, doi:10.5194/bg-11-5087-2014, 2014. 10820
- Bond, T. C., Doherty, S. J., Fahey, D. W., Forster, P. M., Berntsen, T., DeAngelo, B. J., Flanner, M. G., Ghan, S., Kärcher, B., Koch, D., Kinne, S., Kondo, Y., Quinn, P. K., Sarofim, M. C., Schultz, M. G., Schulz, M., Venkataraman, C., Zhang, H., Zhang, S., Bellouin, N., Gutikunda, S. K., Hopke, P. K., Jacobson, M. Z., Kaiser, J. W., Klimont, Z., Lohmann, U., Schwarz, J. P., Shindell, D. T., Storelvmo, T., Warren, S. G., and Zender, C. S.: Bounding the role of black carbon in the climate system: a scientific assessment, *J. Geophys. Res.-Atmos.*, 118, 5380–5552, 2013. 10818
- Bond, W. J., Woodward, F. I., and Midgley, G. F.: The global distribution of ecosystems in a world without fire, *New Phytol.*, 165, 525–538, 2005. 10819
- Bowman, D. M. J. S., Balch, J. K., Artaxo, P., Bond, W. J., Cochrane, M. A., D'antonio, C. M., DeFries, R., Johnston, F. H., Keeley, J. E., and Krawchuk, M. A.: The human dimension of fire regimes on Earth, *J. Biogeogr.*, 38, 2223–2236, 2011. 10819

Quantifying regional, time-varying effects of cropland

S. S. Rabin et al.

Title Page

Abstract

Introduction

Conclusions

References

Tables

Figures



Back

Close

Full Screen / Esc

Printer-friendly Version

Interactive Discussion



Quantifying regional, time-varying effects of cropland

S. S. Rabin et al.

Title Page

Abstract

Introduction

Conclusions

References

Tables

Figures



Back

Close

Full Screen / Esc

Printer-friendly Version

Interactive Discussion



- Cheney, P. and Sullivan, A.: Grassfires: Fuel, Weather and Fire Behaviour, 2nd edn., CSIRO Publishing, Collingwood, Victoria, Australia, 2009. 10828
- Cochrane, M. A. and Schulze, M. D.: Forest fires in the Brazilian Amazon, *Conserv. Biol.*, 12, 948–950, 1998. 10823
- 5 Cox, P. M., Harris, P. P., Huntingford, C., Betts, R. A., Collins, M., Jones, C. D., Jupp, T. E., Marengo, J. A., and Nobre, C. A.: Increasing risk of Amazonian drought due to decreasing aerosol pollution, *Nature*, 453, 212–215, 2008. 10819
- Crutzen, P. J. and Andreae, M. O.: Biomass burning in the tropics: impact on atmospheric chemistry and biogeochemical cycles, *Science*, 250, 1669–1678, 1990. 10819
- 10 FAO: Concepts and Definitions, available at: <http://faostat.fao.org/site/375/default.aspx>, 2005, last access: 18 June 2015. 10826
- Friedl, M., McIver, D., Hodges, J., Zhang, X., Muchoney, D., Strahler, A., Woodcock, C., Gopal, S., Schneider, A., Cooper, A., Baccini, A., Gao, F., and Schaaf, C.: Global land cover mapping from MODIS: algorithms and early results, *Remote Sens. Environ.*, 83, 287–302, 2002. 10825
- 15 Friedl, M. A., Sulla-Menashe, D., Tan, B., Schneider, A., Ramankutty, N., Sibley, A., and Huang, X.: MODIS Collection 5 global land cover: algorithm refinements and characterization of new datasets, *Remote Sens. Environ.*, 114, 168–182, 2010. 10828
- Giglio, L.: MODIS Collection 5 Active Fire Product User's Guide Version 2.5, available at: https://earthdata.nasa.gov/files/MODIS_Fire_Users_Guide_2.5.pdf, 2013, last access: 18 June 2015. 10832
- 20 Giglio, L., van der Werf, G. R., Randerson, J. T., Collatz, G. J., and Kasibhatla, P.: Global estimation of burned area using MODIS active fire observations, *Atmos. Chem. Phys.*, 6, 957–974, doi:10.5194/acp-6-957-2006, 2006. 10824, 10840, 10841
- 25 Giglio, L., Loboda, T., Roy, D. P., Quayle, B., and Justice, C. O.: An active-fire based burned area mapping algorithm for the MODIS sensor, *Remote Sens. Environ.*, 113, 408–420, 2009. 10832
- Giglio, L., Randerson, J. T., van der Werf, G. R., Kasibhatla, P. S., Collatz, G. J., Morton, D. C., and DeFries, R. S.: Assessing variability and long-term trends in burned area by merging multiple satellite fire products, *Biogeosciences*, 7, 1171–1186, doi:10.5194/bg-7-1171-2010, 2010. 10820, 10824
- 30 Hurtt, G. C., Chini, L. P., Frohling, S., Betts, R. A., Feddema, J., Fischer, G., Fisk, J. P., Hibbard, K., Houghton, R. A., Janetos, A., Jones, C. D., Kindermann, G., Kinoshita, T.,

Quantifying regional, time-varying effects of cropland

S. S. Rabin et al.

Title Page

Abstract

Introduction

Conclusions

References

Tables

Figures



Back

Close

Full Screen / Esc

Printer-friendly Version

Interactive Discussion



Klein Goldewijk, K., Riahi, K., Shevliakova, E., Smith, S., Stehfest, E., Thomson, A., Thornton, P., van Vuuren, D. P., and Wang, Y. P.: Harmonization of land-use scenarios for the period 1500–2100: 600 years of global gridded annual land-use transitions, wood harvest, and resulting secondary lands, *Climatic Change*, 109, 117–161, 2011. 10825

5 Klein Goldewijk, K., van Drecht, G., and Bouwman, A. F.: Mapping contemporary global cropland and grassland distributions on a 5x5 minute resolution, *Journal of Land Use Science*, 2, 167–190, 2007. 10826, 10828, 10832

Klein Goldewijk, K., Beusen, A., Van Drecht, G., and De Vos, M.: The HYDE 3.1 spatially explicit database of human-induced global land-use change over the past 12,000 years, *Global Ecol. Biogeogr.*, 20, 73–86, 2010. 10820, 10823, 10825, 10832

10 Korontzi, S., McCarty, J., Loboda, T., Kumar, S., and Justice, C.: Global distribution of agricultural fires in croplands from 3 years of Moderate Resolution Imaging Spectroradiometer (MODIS) data, *Global Biogeochem. Cy.*, 20, GB2021, doi:10.1029/2005GB002529, 2006. 10820

15 Laris, P.: Burning the seasonal mosaic: preventative burning strategies in the wooded savanna of southern Mali, *Hum. Ecol.*, 30, 155–186, 2002. 10820

Le Page, Y., Oom, D., Silva, J. M. N., Jönsson, P., and Pereira, J. M. C.: Seasonality of vegetation fires as modified by human action: observing the deviation from eco-climatic fire regimes, *Global Ecol. Biogeogr.*, 19, 575–588, 2010. 10819

20 Le Page, Y., Morton, D., Bond-Lamberty, B., Pereira, J. M. C., and Hurtt, G.: HESFIRE: a global fire model to explore the role of anthropogenic and weather drivers, *Biogeosciences*, 12, 887–903, doi:10.5194/bg-12-887-2015, 2015. 10820

Lenihan, J., Daly, C., Bachelet, D., and Neilson, R.: Simulating broad-scale fire severity in a dynamic global vegetation model, *Northwest Sci.*, 72, 91–101, 1998. 10820

25 Li, F., Levis, S., and Ward, D. S.: Quantifying the role of fire in the Earth system – Part 1: Improved global fire modeling in the Community Earth System Model (CESM1), *Biogeosciences*, 10, 2293–2314, doi:10.5194/bg-10-2293-2013, 2013. 10820, 10834

Magi, B. I., Rabin, S., Shevliakova, E., and Pacala, S.: Separating agricultural and non-agricultural fire seasonality at regional scales, *Biogeosciences*, 9, 3003–3012, doi:10.5194/bg-9-3003-2012, 2012. 10819, 10821, 10824

30 Marlon, J., Bartlein, P. J., Carcaillet, C., Gavin, D. G., Harrison, S. P., Higuera, P. E., Joos, F., Power, M. J., and Prentice, I. C.: Climate and human influences on global biomass burning over the past two millennia, *Nat. Geosci.*, 1, 697–702, 2008. 10819

Quantifying regional, time-varying effects of cropland

S. S. Rabin et al.

[Title Page](#)

[Abstract](#)

[Introduction](#)

[Conclusions](#)

[References](#)

[Tables](#)

[Figures](#)



[Back](#)

[Close](#)

[Full Screen / Esc](#)

[Printer-friendly Version](#)

[Interactive Discussion](#)



Myhre, G., Shindell, D. T., Bréon, F.-M., Collins, W., Fuglestvedt, J., Huang, J., Koch, D., Lamarque, J.-F., Lee, D., Mendoza, B., Nakajima, T., Robock, A., Stephens, G., and Zhang, H.: Anthropogenic and Natural Radiative Forcing, Cambridge University Press, Cambridge, UK and New York, NY, USA, 659–740, 2013. 10819

5 Olson, D. M., Dinerstein, E., Wikramanayake, E. D., Burgess, N. D., Powell, G. V., Underwood, E. C., D'amico, J. A., Itoua, I., Strand, H. E., and Morrison, J. C.: Terrestrial ecoregions of the world: a new map of life on Earth: a new global map of terrestrial ecoregions provides an innovative tool for conserving biodiversity, *Bioscience*, 51, 933–938, 2001. 10823

10 Pechony, O. and Shindell, D. T.: Fire parameterization on a global scale, *J. Geophys. Res.*, 114, D16115, doi:10.1029/2009JD011927, 2009. 10820

Pfeiffer, M., Spessa, A., and Kaplan, J. O.: A model for global biomass burning in preindustrial time: LPJ-LMfire (v1.0), *Geosci. Model Dev.*, 6, 643–685, doi:10.5194/gmd-6-643-2013, 2013. 10820, 10834

15 Prentice, I. C., Kelley, D. I., Foster, P. N., Friedlingstein, P., Harrison, S. P., and Bartlein, P. J.: Modeling fire and the terrestrial carbon balance, *Global Biogeochem. Cy.*, 25, GB3005, doi:10.1029/2010GB003906, 2011. 10820

Pyne, S. J., Andrews, P. L., and Laven, R. D.: Fire and culture, in: *Introduction to Wildland Fire*, John Wiley and Sons, New York, 213–307, 1996a. 10819

20 Pyne, S. J., Andrews, P. L., and Laven, R. D.: Fire ecology, in: *Introduction to Wildland Fire*, John Wiley and Sons, New York, 171–212, 1996b. 10819

Randerson, J. T., Chen, Y., van der Werf, G. R., Rogers, B. M., and Morton, D. C.: Global burned area and biomass burning emissions from small fires, *J. Geophys. Res.*, 117, G04012, doi:doi:10.1029/2012JG002128, 2012. 10818, 10823, 10824, 10825, 10832

25 Scott, A. C., Bowman, D. M. J. S., Bond, W. J., Pyne, S., and Alexander, M. E.: Pyrogeography—temporal and spatial patterns of fire, in: *Fire on Earth: An Introduction*, John Wiley & Sons, West Sussex, UK, 113–129, 2014. 10819

Seiler, W. and Crutzen, P. J.: Estimates of gross and net fluxes of carbon between the biosphere and the atmosphere from biomass burning, *Climatic Change*, 2, 207–247, 1980. 10827

30 Taylor, K. E., Stouffer, R. J., and Meehl, G. A.: An overview of CMIP5 and the experiment design, *B. Am. Meteorol. Soc.*, 93, 485–498, 2012. 10825

Thonicke, K., Spessa, A., Prentice, I. C., Harrison, S. P., Dong, L., and Carmona-Moreno, C.: The influence of vegetation, fire spread and fire behaviour on biomass burning and

trace gas emissions: results from a process-based model, *Biogeosciences*, 7, 1991–2011, doi:10.5194/bg-7-1991-2010, 2010. 10820

Uhl, C. and Buschbacher, R.: A disturbing synergism between cattle ranch burning practices and selective tree harvesting in the eastern Amazon, *Biotropica*, 17, 265–268, 1985. 10819, 10823

Venevsky, S., Thonicke, K., Sitch, S., and Cramer, W.: Simulating fire regimes in human-dominated ecosystems: Iberian Peninsula case study, *Glob. Change Biol.*, 8, 984–998, 2002. 10820

Ward, D. S., Kloster, S., Mahowald, N. M., Rogers, B. M., Randerson, J. T., and Hess, P. G.: The changing radiative forcing of fires: global model estimates for past, present and future, *Atmos. Chem. Phys.*, 12, 10857–10886, doi:10.5194/acp-12-10857-2012, 2012. 10819

Yevich, R. and Logan, J. A.: An assessment of biofuel use and burning of agricultural waste in the developing world, *Global Biogeochem. Cy.*, 17, 1095, doi:10.1029/2002GB001952, 2003. 10819

BGD

12, 10817–10855, 2015

Quantifying regional, time-varying effects of cropland

S. S. Rabin et al.

Title Page

Abstract

Introduction

Conclusions

References

Tables

Figures

◀

▶

◀

▶

Back

Close

Full Screen / Esc

Printer-friendly Version

Interactive Discussion



BGD

12, 10817–10855, 2015

Quantifying regional,
time-varying effects
of cropland

S. S. Rabin et al.

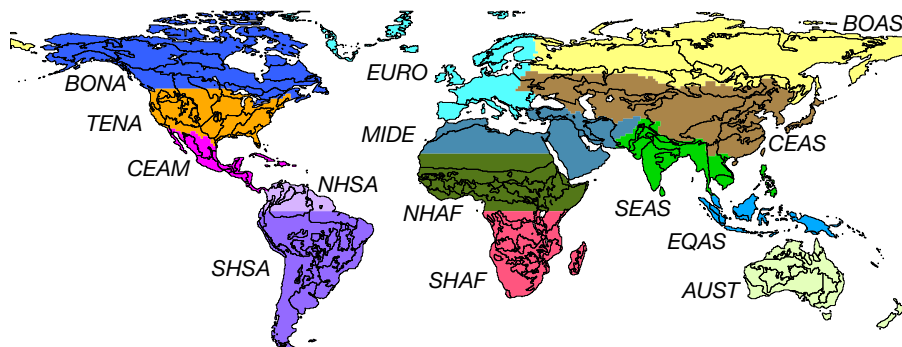


Figure 1. Regions used for analysis (outlines) overlaid on GFED regions (colors and labels; Giglio et al., 2006). See Table 1 for abbreviations.

Title Page

Abstract

Introduction

Conclusions

References

Tables

Figures



Back

Close

Full Screen / Esc

Printer-friendly Version

Interactive Discussion



Quantifying regional, time-varying effects of cropland

S. S. Rabin et al.

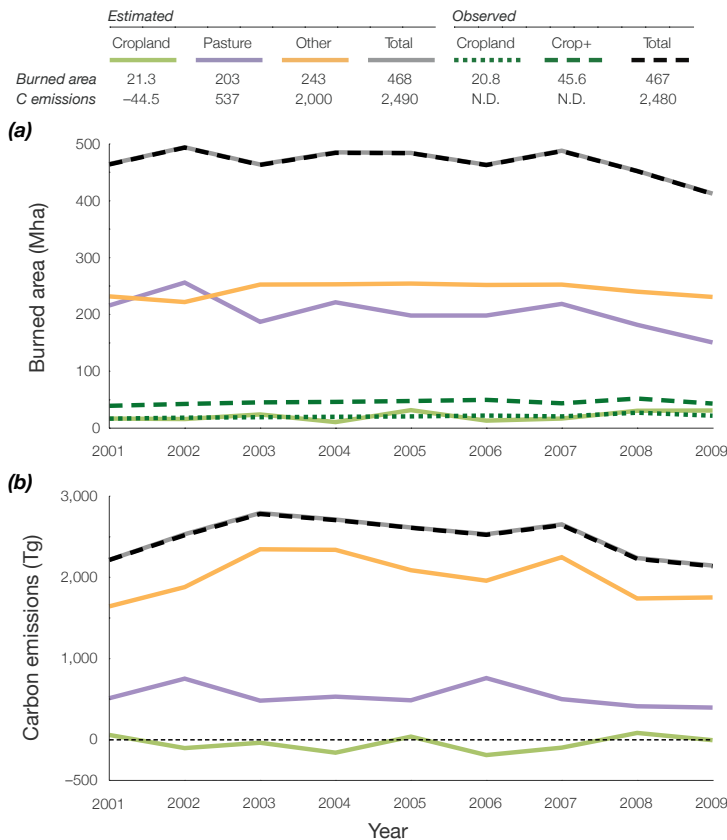


Figure 2. Observed and estimated annual timeseries of net observed and estimated global burned area (a, Mha) and C emissions (b, Tg = Mt). Numbers in table represent annual means. “N.D.” = no data; “Crop+” = cropland + cropland-natural mosaic. Corresponds to Fig. A1 in Appendix A.

[Title Page](#)

[Abstract](#) [Introduction](#)
[Conclusions](#) [References](#)
[Tables](#) [Figures](#)

◀ ▶
◀ ▶

[Back](#) [Close](#)

[Full Screen / Esc](#)

[Printer-friendly Version](#)

[Interactive Discussion](#)



Quantifying regional, time-varying effects of cropland

S. S. Rabin et al.

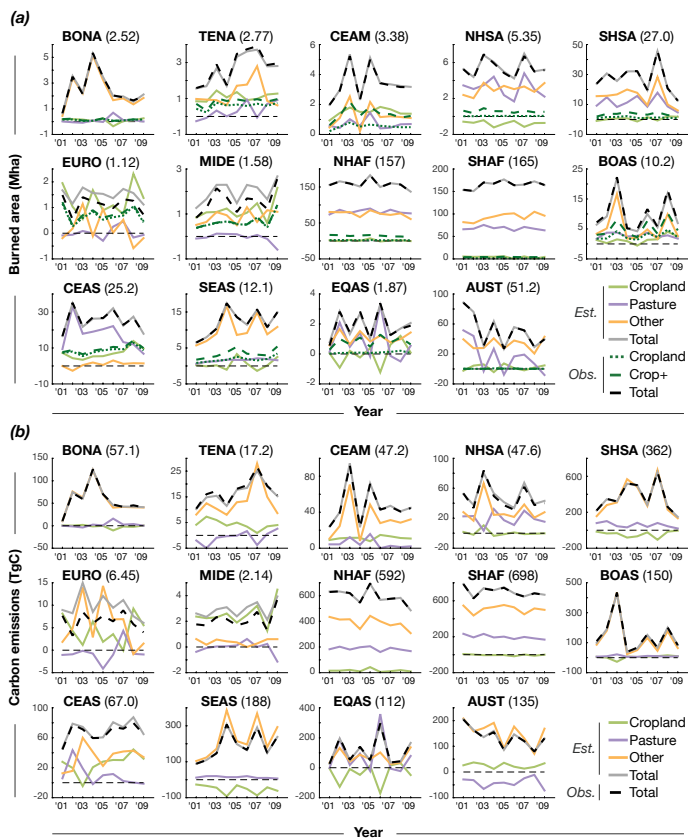


Figure 3. Annual timeseries of different fire types in each GFED region based on analysis of burned area (**a**; Mha) and C emissions (**b**; TgC). Numbers in parentheses next to region names represent mean annual observed fire there (either burned area or C emissions). Corresponds to Fig. A2 in Appendix A.

Title Page

Abstract Introduction

Conclusions References

Tables Figures

◀ ▶

◀ ▶

Back Close

Full Screen / Esc

Printer-friendly Version

Interactive Discussion



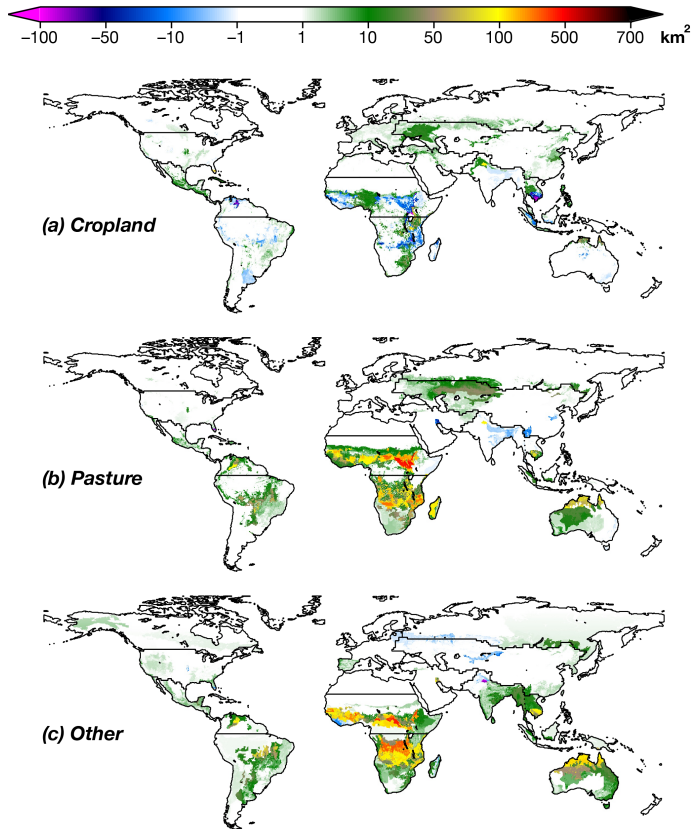


Figure 4. Maps of mean annual burned area (km^2) associated with **(a)** cropland, **(b)** pasture, and **(c)** other land. Numbers can be interpreted as how much more (or less) fire would be expected if the area of the given land cover were to double (and the others remain the same). Corresponds to Fig. A3 in Appendix A.

Quantifying regional, time-varying effects of cropland

S. S. Rabin et al.

Title Page

Abstract

Introduction

Conclusions

References

Tables

Figures

◀

▶

◀

▶

Back

Close

Full Screen / Esc

Printer-friendly Version

Interactive Discussion



Quantifying regional,
time-varying effects
of cropland

S. S. Rabin et al.

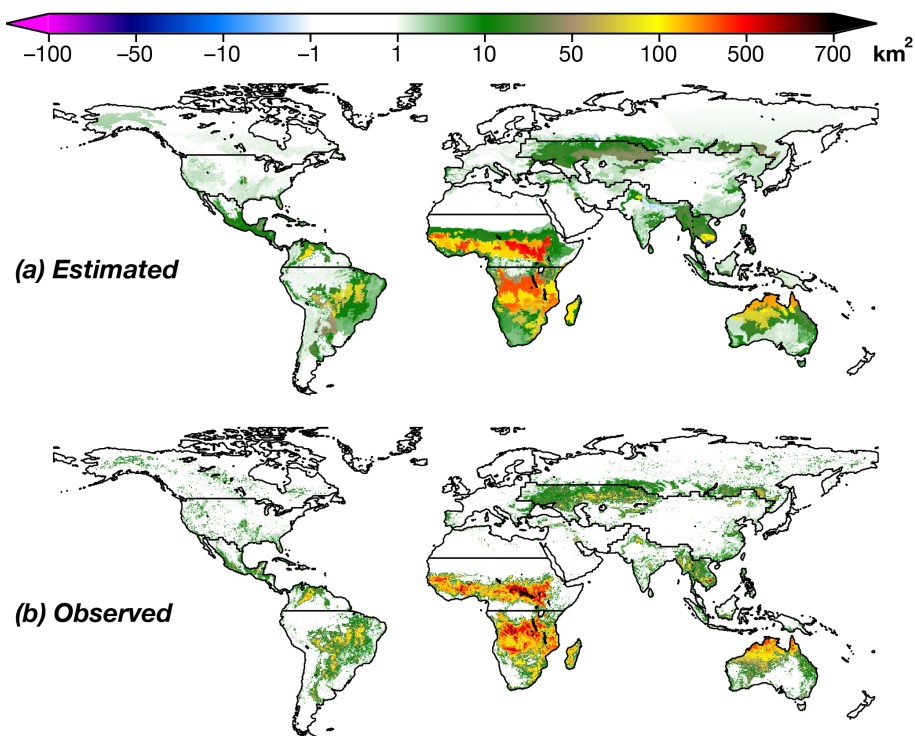


Figure 5. Maps of net mean annual total burned area (km^2): **(a)** Estimated. **(b)** Observed. Corresponds to Fig. A4 in Appendix A.

[Title Page](#)[Abstract](#)[Introduction](#)[Conclusions](#)[References](#)[Tables](#)[Figures](#)[Back](#)[Close](#)[Full Screen / Esc](#)[Printer-friendly Version](#)[Interactive Discussion](#)

Quantifying regional, time-varying effects of cropland

S. S. Rabin et al.

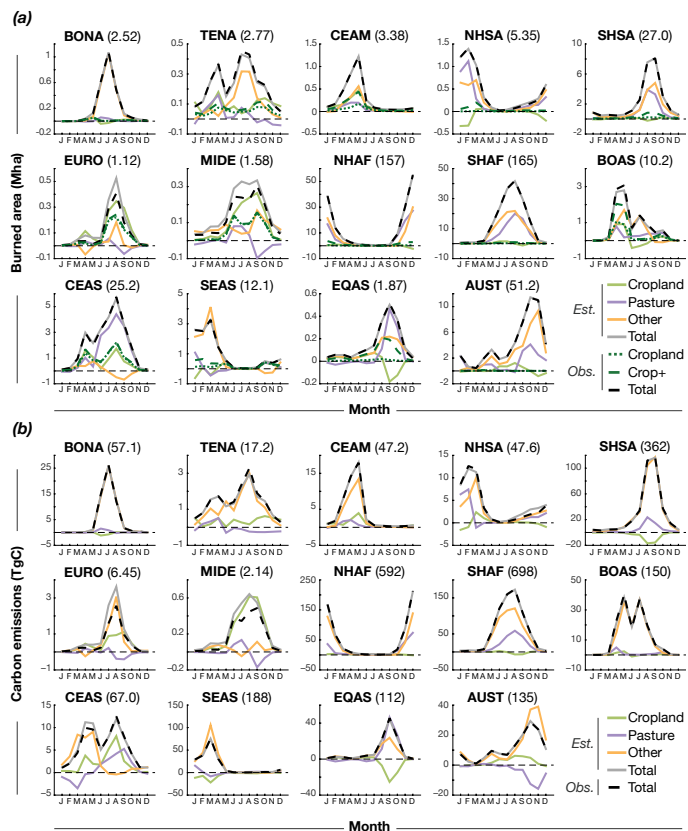


Figure 6. Seasonality of different fire types in each GFED region based on analysis of burned area (**a**; Mha) and C emissions (**b**; TgC). Numbers in parentheses next to region names represent mean annual observed fire there (either burned area or C emissions). Corresponds to Fig. A5 in Appendix A.

Title Page

Abstract

Introduction

Conclusions

References

Tables

Figures



Back

Close

Full Screen / Esc

Printer-friendly Version

Interactive Discussion



BGD

12, 10817–10855, 2015

Quantifying regional, time-varying effects of cropland

S. S. Rabin et al.

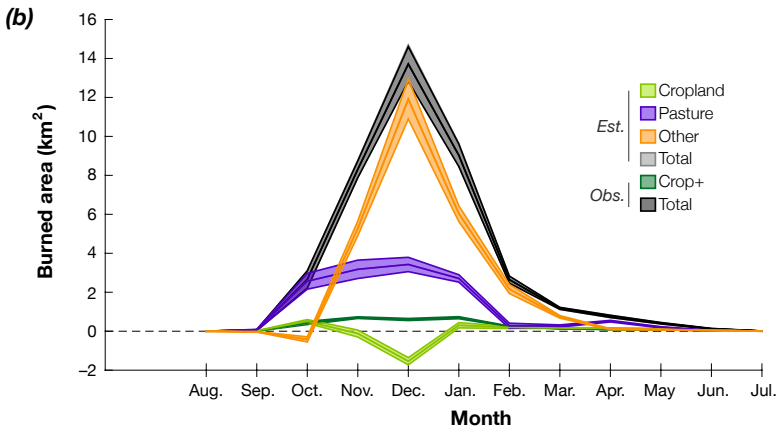
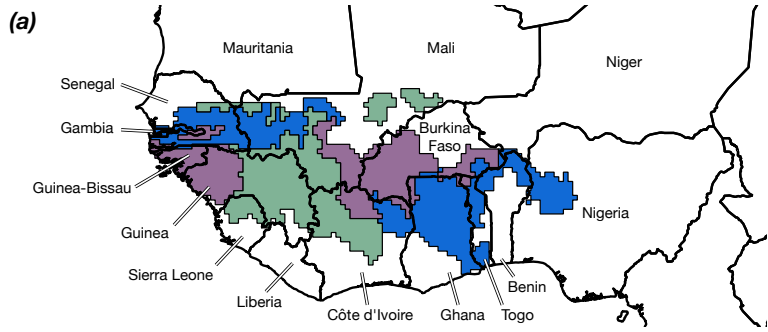


Figure 7. (a) Area included in West African case study. (b) Mean seasonality of burned area in West African case study regions. Shading represents interannual variability (± 1 SEM). Note that the X axis begins in August. Corresponds to Fig. A6 in Appendix A.

Title Page

Abstract Introduction

Conclusions References

Tables Figures

◀ ▶

◀ ▶

Back Close

Full Screen / Esc

Printer-friendly Version

Interactive Discussion



Quantifying regional, time-varying effects of cropland

S. S. Rabin et al.

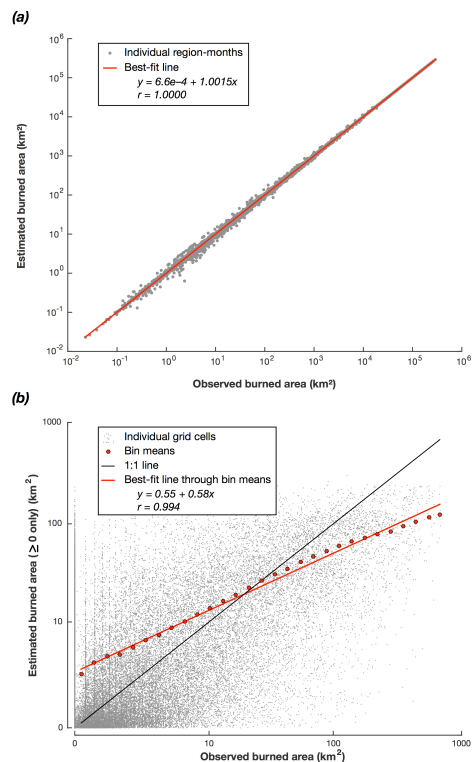


Figure 8. Scatter plots comparing estimated and observed total burned area for **(a)** each analysis region and month (region-month), and **(b)** each grid cell. Values ≤ 0 not shown on scatter plots due to log-scale axes. Grid cells in region-months with no observed fire were excluded, as the analysis was not performed for such points. For **(b)**, regression performed on means of observed and estimated burned area for bins of observed burned area (red points), with minimum 100 grid cells required for a bin to be included. Also for **(b)**, $\frac{1}{75}$ of cells were chosen at random for scatter plotting. Corresponds to Fig. A7 in Appendix A.

[Title Page](#)
[Abstract](#)
[Introduction](#)
[Conclusions](#)
[References](#)
[Tables](#)
[Figures](#)

[Back](#)
[Close](#)
[Full Screen / Esc](#)
[Printer-friendly Version](#)
[Interactive Discussion](#)


Quantifying regional, time-varying effects of cropland

S. S. Rabin et al.

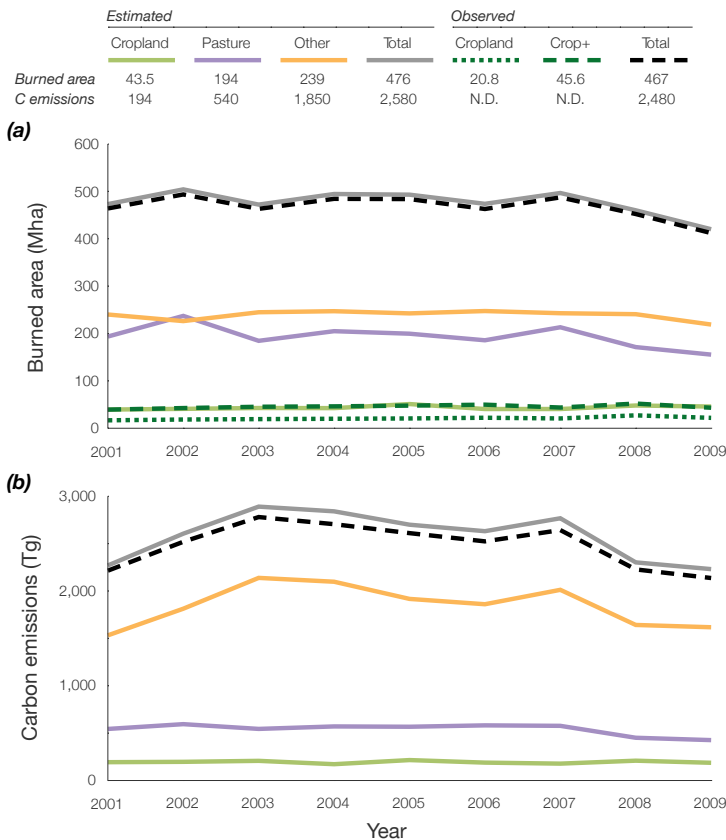


Figure A1. Observed and estimated annual timeseries of net observed and estimated global burned area (a, Mha) and C emissions (b, Tg = Mt) from the constrained- \hat{F}_k analysis. Numbers in table represent annual means. “N.D.” = no data; “Crop+” = cropland + cropland-natural mosaic. Corresponds to Fig. 2 in main text.

[Title Page](#)

[Abstract](#) [Introduction](#)

[Conclusions](#) [References](#)

[Tables](#) [Figures](#)

[◀](#) [▶](#)

[◀](#) [▶](#)

[Back](#) [Close](#)

[Full Screen / Esc](#)

[Printer-friendly Version](#)

[Interactive Discussion](#)



Quantifying regional, time-varying effects of cropland

S. S. Rabin et al.

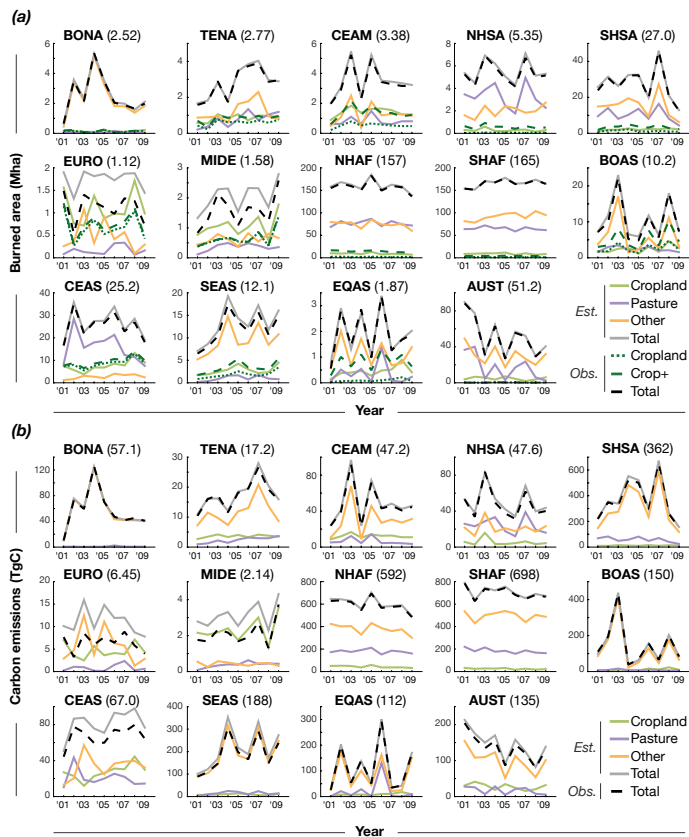


Figure A2. Annual timeseries of different fire types in each GFED region based on constrained- \hat{F}_k analysis of burned area (**a**; Mha) and C emissions (**b**; TgC). Numbers in parentheses next to region names represent mean annual observed fire there (either burned area or C emissions). Corresponds to Fig. 3 in main text.

Title Page

Abstract Introduction

Conclusions References

Tables Figures

◀ ▶

◀ ▶

Back Close

Full Screen / Esc

Printer-friendly Version

Interactive Discussion



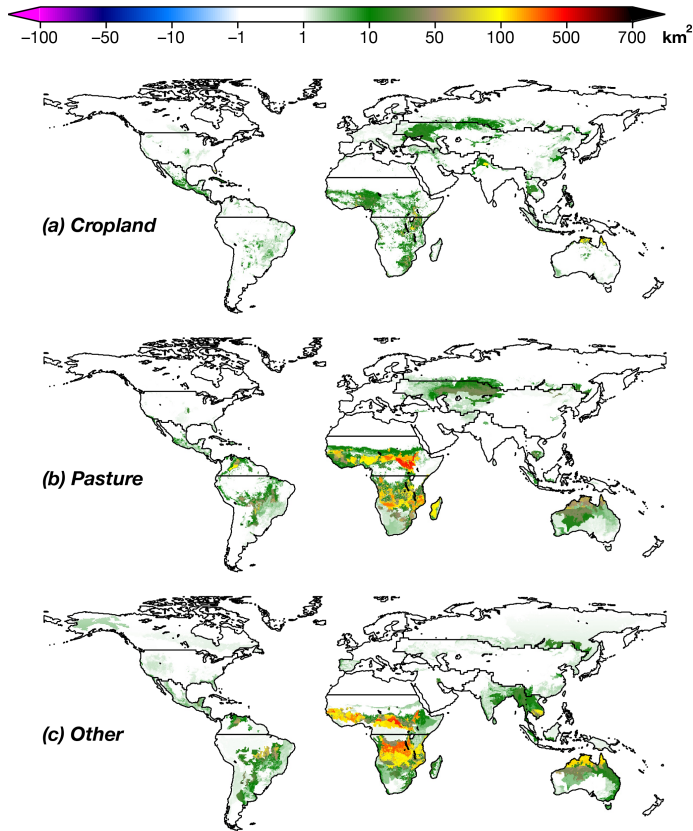


Figure A3. Maps, from constrained- \hat{F}_k analysis, of mean annual burned area (km^2) associated with (a) cropland, (b) pasture, and (c) other land. Numbers can be interpreted as how much more (or less) fire would be expected if the area of the given land cover were to double (and the others remain the same). Corresponds to Fig. 4 in main text.

Quantifying regional, time-varying effects of cropland

S. S. Rabin et al.

Title Page	
Abstract	Introduction
Conclusions	References
Tables	Figures
◀	▶
◀	▶
Back	Close
Full Screen / Esc	
Printer-friendly Version	
Interactive Discussion	



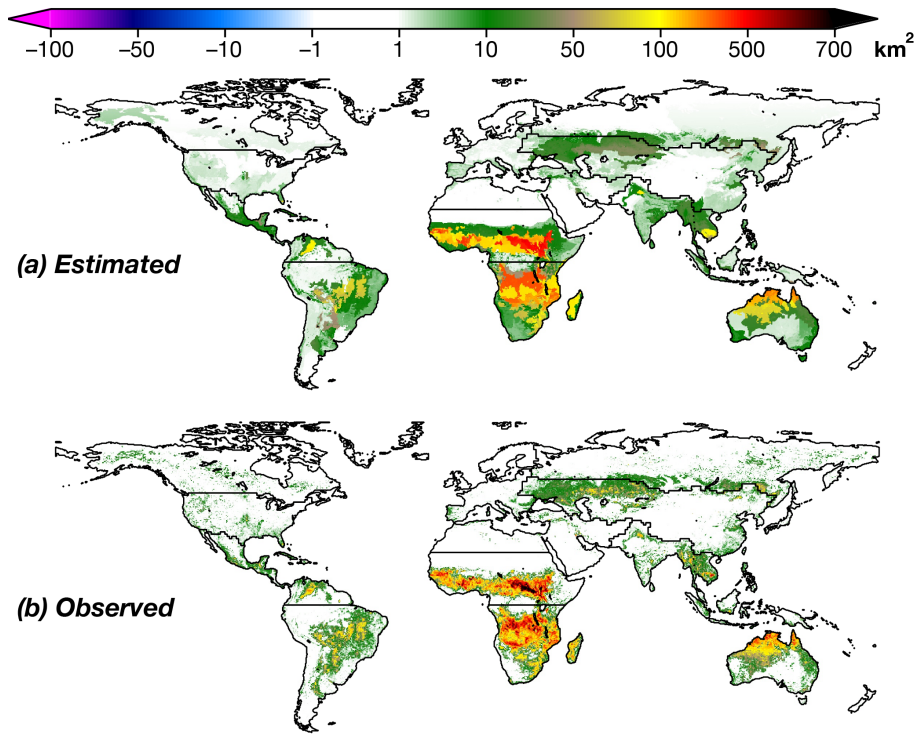


Figure A4. Maps of mean annual total burned area (km²): **(a)** Estimated by constrained- \hat{F}_k analysis. **(b)** Observed. Corresponds to Fig. 5 in main text.

Quantifying regional, time-varying effects of cropland

S. S. Rabin et al.

Title Page

Abstract

Introduction

Conclusions

References

Tables

Figures

◀

▶

◀

▶

Back

Close

Full Screen / Esc

Printer-friendly Version

Interactive Discussion



Quantifying regional, time-varying effects of cropland

S. S. Rabin et al.

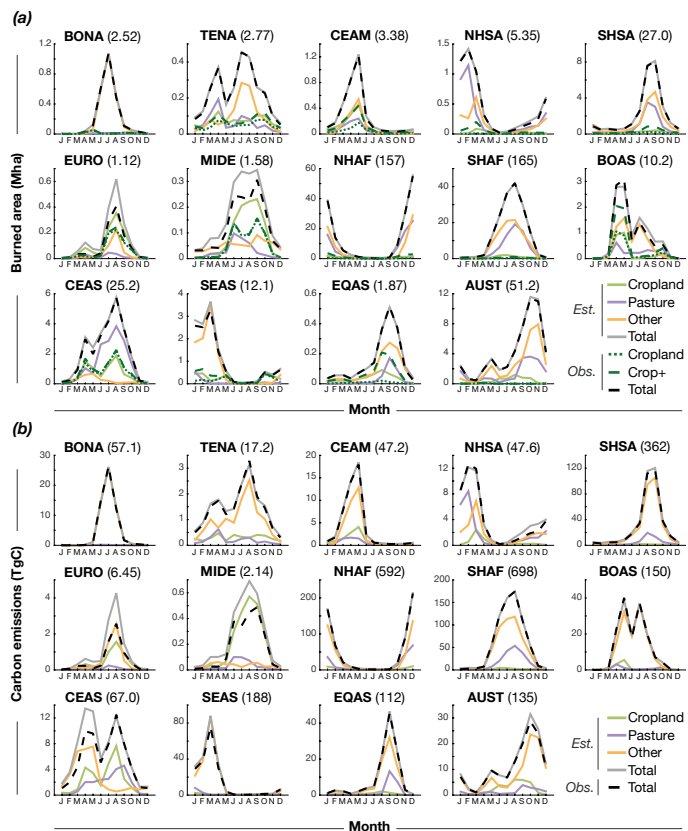


Figure A5. Seasonality of different fire types in each GFED region based on constrained- \hat{F}_k analysis of burned area (**a**; Mha) and C emissions (**b**; TgC). Numbers in parentheses next to region names represent mean annual observed fire there (either burned area or C emissions). Corresponds to Fig. 6 in main text.

Title Page

Abstract Introduction

Conclusions References

Tables Figures

◀ ▶

◀ ▶

Back Close

Full Screen / Esc

Printer-friendly Version

Interactive Discussion



Quantifying regional, time-varying effects of cropland

S. S. Rabin et al.

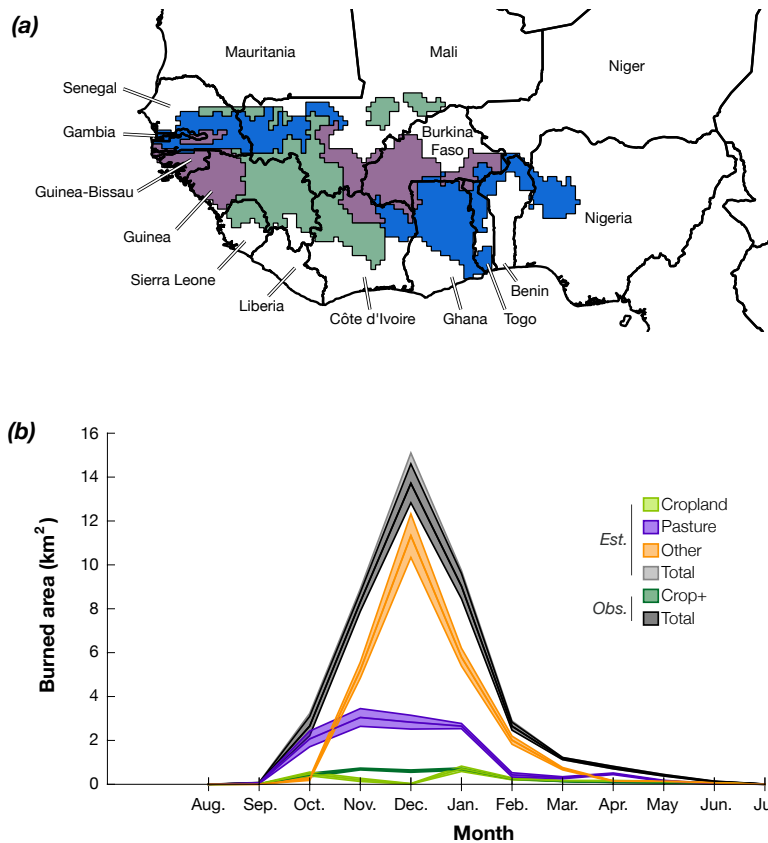


Figure A6. Mean seasonality of burned area in West African case study regions based on constrained- \hat{F}_k analysis. Shading represents interannual variability (± 1 SEM). Note that the X axis begins in August. Corresponds to Fig. 7 in main text.

[Title Page](#)

[Abstract](#) | [Introduction](#)

[Conclusions](#) | [References](#)

[Tables](#) | [Figures](#)

[◀](#) | [▶](#)

[◀](#) | [▶](#)

[Back](#) | [Close](#)

[Full Screen / Esc](#)

[Printer-friendly Version](#)

[Interactive Discussion](#)



Quantifying regional,
time-varying effects
of cropland

S. S. Rabin et al.

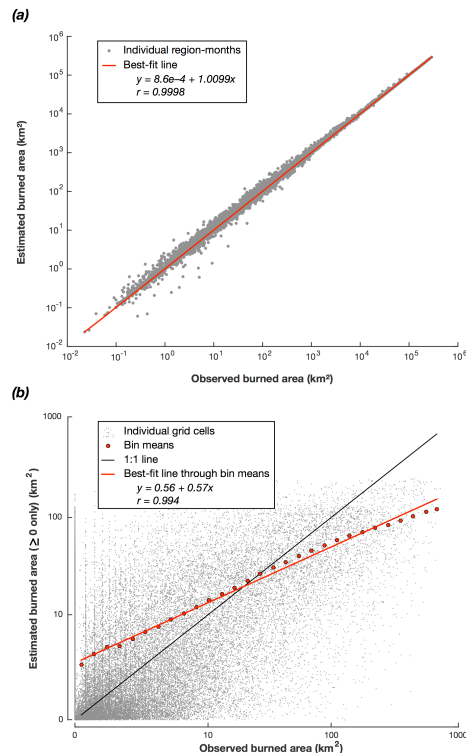


Figure A7. Scatter plots comparing estimated burned area from constrained- \hat{F}_k analysis with observations for **(a)** each analysis region and month (region-month), and **(b)** each grid cell. Values ≤ 0 not shown on scatter plots due to log-scale axes. (Gridcells in) region-months with no observed fire were excluded, as the analysis was not performed for such points. For **(b)**, regression performed on means of observed and estimated burned area for bins of observed burned area (red points), with minimum 100 grid cells required for a bin to be included. Also for **(b)**, $\frac{1}{75}$ of cells were chosen at random for scatter plotting. Corresponds to Fig. 8 in main text.

Title Page

Abstract

Introduction

Conclusions

References

Tables

Figures



Back

Close

Full Screen / Esc

Printer-friendly Version

Interactive Discussion

